

Dynamical masses of young star clusters in interacting galaxies

Sabine Mengel^a, Matt D. Lehnert,^b Niranjana A. Thatte^b and Reinhard Genzel^b

^aLeiden Observatory, P.O. Box 9513, NL-2300 RA Leiden, The Netherlands

^bMax-Planck-Institut für extraterrestrische Physik, Giessenbachstr., 85748 Garching, Germany

ABSTRACT

Using ISAAC on VLT-ANTU and UVES on VLT-KUEYEN we have begun a program to measure stellar velocity dispersions of young star clusters in merging and interacting galaxies. In this contribution, we present results for clusters in two interacting galaxies – NGC 4038/39 and NGC 1487. Combining the measured velocity dispersions with sizes of the clusters estimated from Hubble Space Telescope imaging data resulted in the first determinations of dynamical masses of stellar clusters in galaxy mergers. Due to the faintness of the clusters and the high spectral resolution required, these results could only be obtained in with 10m class telescopes.

Our results suggest that masses, sizes and concentrations of the light distributions are comparable to those of globular clusters, supporting the idea that part of the globular cluster population in elliptical galaxies is formed as a result of a merger event between two gas-rich spiral galaxies. However, the initial mass function (IMF) of the stars in the clusters seems to vary with environment: In some regions (dust-rich?), the IMF is more biased towards low-mass stars than in other (dust-poor) regions. There is a long-standing and substantial controversy in the literature whether or not there exists a "universal IMF". Our results for clusters in merging galaxies support the notion that the IMF depends on the birth environment of the cluster or perhaps some other variable. The relative content of low mass stars also influences the survival probability of stellar clusters. For their masses and light concentrations, some of the clusters have sufficiently shallow IMFs that it is likely that they will dissolve within a Hubble time, while for others, the IMF is sufficiently steep that they are likely to survive but undergo significant mass loss during their evolution.

Keywords: young star clusters, merging galaxies, dynamical masses, IMF

1. INTRODUCTION

Even though the idea has been around for more than ten years, the question has not yet been answered conclusively whether the merger of two late-type galaxies leads to the formation of an early type galaxy, and whether the large numbers of young star clusters seen in these mergers¹²³⁴⁵⁶ will evolve into globular clusters, comparable to at least part of the populations of globular clusters seen in present-day elliptical galaxies. One way of attempting to answer this question is to determine properties of many individual star clusters in various merging galaxies, thereby sampling different physical environments. The properties of these individual clusters can then be compared with those of globular clusters (GCs) in nearby galaxies. The dynamical cluster mass is a critical parameter in combination with age and luminosity, because it reveals the presence or absence of low-mass stars, which are too faint to contribute significantly to the luminosity of the cluster, but heavily influence its survival probability. For example, a cluster with size and mass comparable to that of a GC, but for example a lower mass cutoff in the IMF of $2 M_{\odot}$, will never survive a Hubble time.⁷

With these arguments in mind, we have begun a program to obtain dynamical mass and size estimates of young compact clusters in a sample of nearby merging galaxies. Here we present data for two merging galaxies: NGC 4038/39 and NGC 1487. The most challenging aspect of this project lies in the determination of cluster masses:

In order to obtain dynamical cluster masses, the stellar velocity dispersion in the cluster needs to be determined, which is typically around 15 km s^{-1} and therefore requires high spectral resolution of these faint targets, which is only achievable with 10m class telescopes. The second parameter required for the mass is an

estimate of the cluster size, which for objects at distances between 10 and 20 Mpc and sizes of 2-4 pc requires high spatial resolution which generally requires Hubble Space Telescope observations.

Our high resolution spectroscopy was performed using the optical echelle spectrograph, UVES, and the infrared imager and spectrometer, ISAAC, on VLT-KUEYEN and VLT-ANTU, respectively, during several runs in 2000 and 2001. For size estimates, we used archival HST images of both, NGC 4038/39 and NGC 1487. However, we just obtained HST-ACS images of NGC 1487 with which we hope to greatly improve the size estimates for those clusters.

Globular clusters have a typical mass of $1-2 \times 10^5 M_{\odot}$ and a mass function which is log-normal.⁸ The population of clusters in NGC 4038/4039 (“the Antennae”), however, has a power law luminosity function, and the same shape is also suggested for the mass function^{5,9}. Masses determined from photometric data are as large as a few $\times 10^6 M_{\odot}$ for some of the few thousand clusters^{9,10} and the determined ages span a large range.^{5,10} No comparable study exists for NGC 1487, which is not equally rich in young clusters, but shows some morphological similarity to the Antennae: It seems to also consist of two merging galaxies and a star forming region located outside both galaxies. The clusters we selected for spectroscopy are located in that region (see Figure 2).

2. OBSERVATIONS

Spectroscopy was performed with ISAAC at VLT-ANTU and UVES at VLT-KUEYEN in 04/2000, 04/2001 and 12/2001. ISAAC was configured to have a $0''.3$ slit and a central wavelength of $2.31 \mu\text{m}$ with a total wavelength coverage from 2.25 to $2.37 \mu\text{m}$. This was sufficient to include the ^{12}CO (2-0) and (3-1) absorption bands and at a resolution, $\lambda/\Delta\lambda \sim 9000$. Observations of late-type supergiant stars were taken so that they could be used as templates for the determination of the velocity dispersions*. Observations were performed by nodding along the slit and dithering the source position from one exposure to the next. Atmospheric calibrator stars were observed several times during the night.

The target clusters were selected using the results from NTT-SOFI imaging observations performed in May 1999 (Mengel et al. 2002, in preparation) and in service mode in 2000 (also NTT-SOFI). They included narrow band imaging in the CO(2-0) band-head and revealed those clusters which are at an age where the near-infrared continuum emission is dominated by red supergiants. This information was also used for the age determination of the clusters in comparison to evolutionary synthesis models (Starburst99 by Leitherer et al.)¹¹ and included additionally equivalent widths in Br γ and the Calcium Triplet (CaT), and several broadband colors.

The selection of clusters dominated by supergiants or similarly cool stars is essential, because very hot young stars do not show atmospheric absorption features, which are required for the determination of the stellar velocity dispersion. Bright clusters with high equivalent width in the CO band-heads were selected, and those which suffered high extinction were preferentially observed with ISAAC. For the locations of observed clusters see Fig. 1 and 2. Their detectability in at least one band from the HST imaging program of Whitmore et al.⁵ was a necessary additional constraint, since the compactness of each cluster means that their radii must be measured from HST data (see §3.4).

The high-resolution optical echelle spectrograph UVES was configured with a slit width of $1''$, which resulted in a resolution of $R \approx 38,000$. A dichroic was placed in the light path allowing the use of both the red and blue arms of the spectrograph. However, in this paper we will discuss only the results obtained with data from the red arm. The central wavelength of the red arm was shifted to 8400\AA since part of the CaT would have fallen right in the small gap between the two CCDs that cover the lower and the upper part of the spectra in the red arm.

One cluster ([W99]-2) was observed with both instruments. Obtaining two independent observations of a cluster provides an independent estimate of the velocity dispersion to test the uncertainties of our measurements and to gauge whether there might be some systematic differences in velocity dispersions determined from the CaT in the optical with UVES versus that obtained from the CO band-head with ISAAC in the near-IR. A range of template supergiants was observed (early K through late M-type supergiant stars), but also several

*This research has made use of the SIMBAD database, operated at CDS, Strasbourg, France

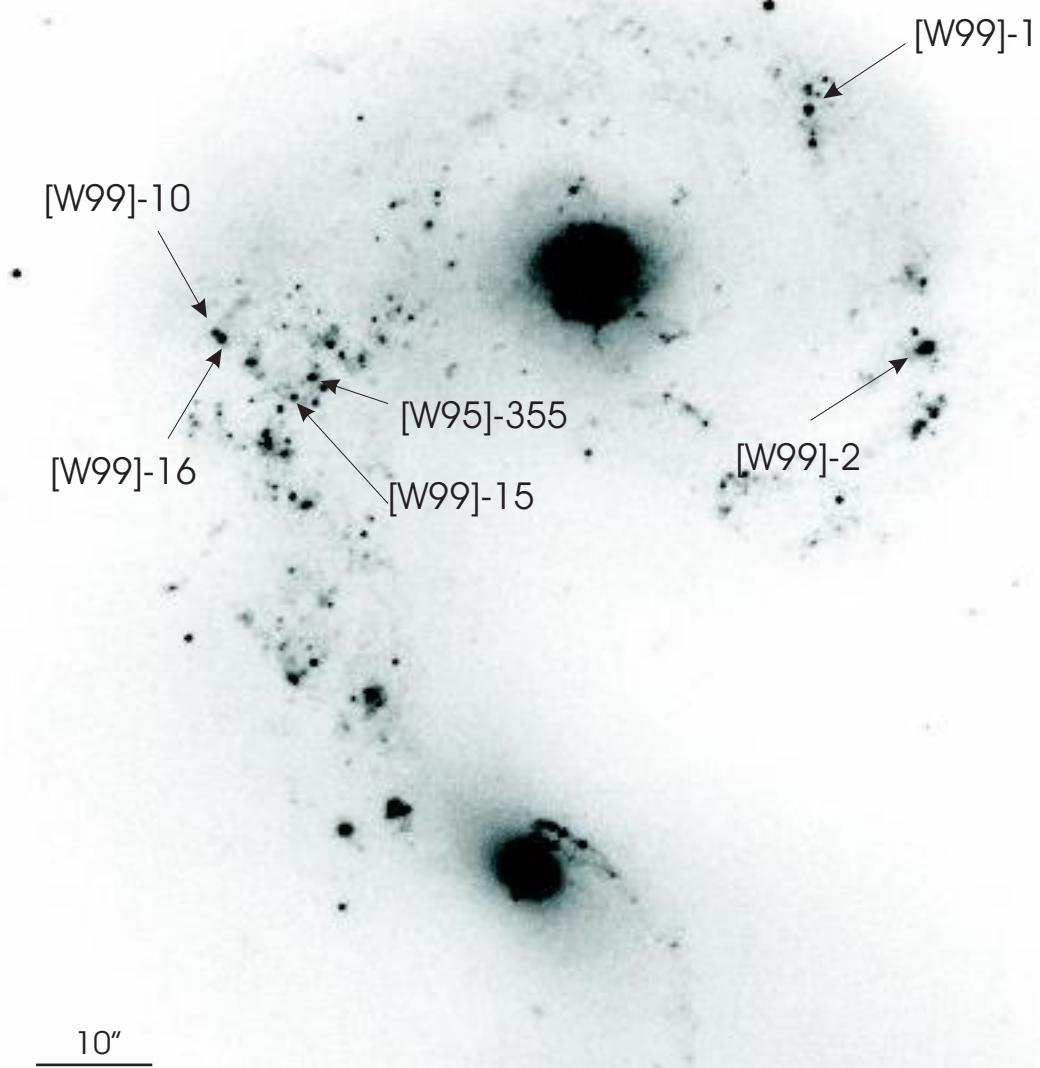


Figure 1. ISAAC K-band image of NGC 4038/39 with indication of clusters with spectroscopy, using the naming convention as in W99.

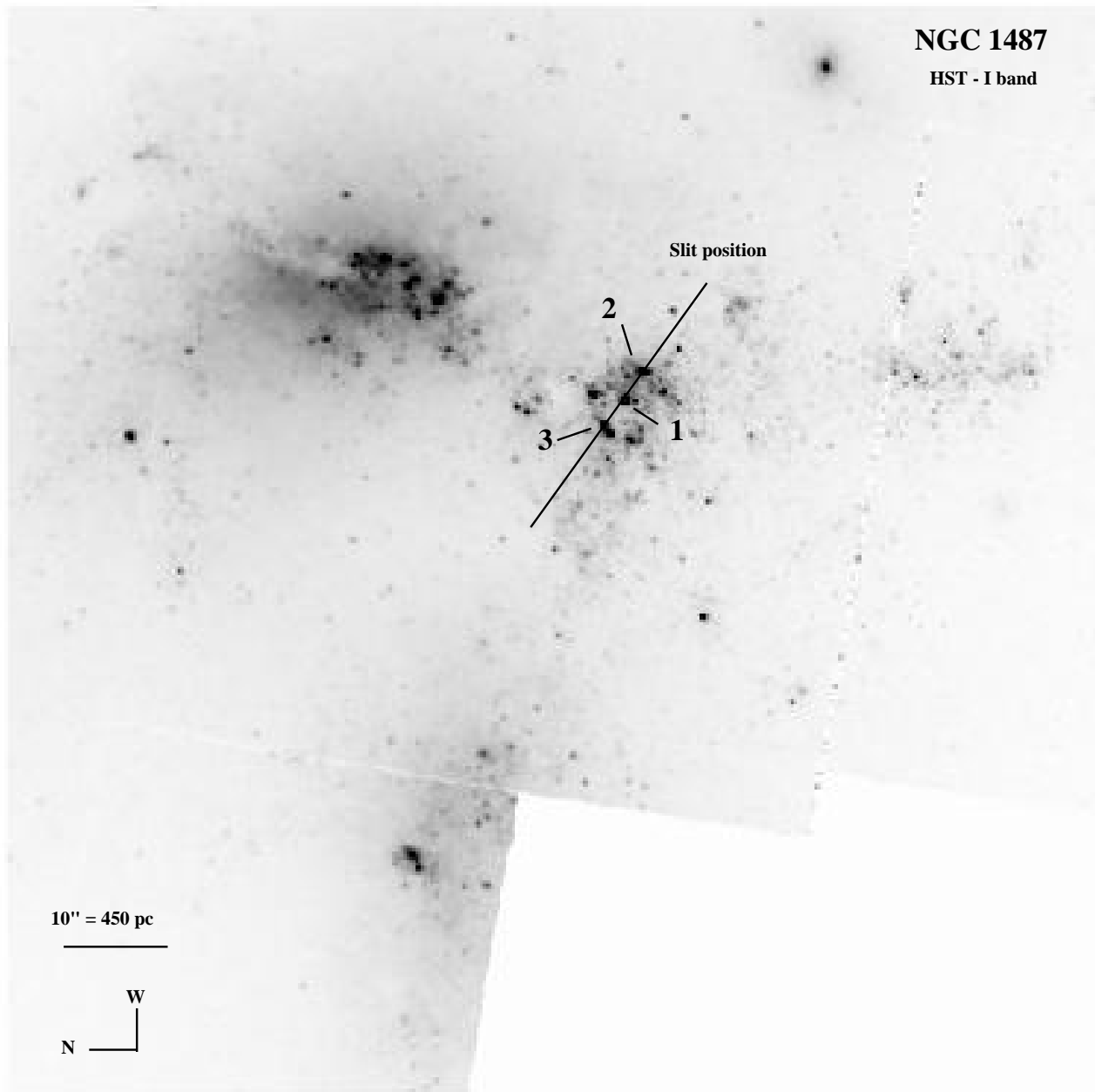


Figure 2. HST I-band image of NGC 1487 with indication of slit position, and the clusters for which we extracted spectra.

hot main sequence stars (late O through mid B-type main sequence stars). Massive main sequence stars are expected to dominate the blue spectrum and to contribute significantly to the flux in the I-band.¹²

3. REDUCTION AND ANALYSIS

3.1. Reduction of the near-IR data

The reduction of ISAAC data was performed in a standard way using the IRAF data reduction package[†]. It included dark subtraction and flat-fielding (using a normalized flat-field created from internal flat observations) on the two-dimensional array. Sky subtraction was performed pairwise, followed by a rejection of cosmic ray hits and bad pixels. The spectra were then corrected for tilt and slit curvature by tracing the peak of the stellar spatial profile along the dispersion direction and fitting a polynomial to the function of displacement versus wavelength. The corresponding procedure was also applied to the orthogonal direction. Single integrations were combined by shifting-and-adding, including a rejection of highest and lowest pixels. The rejection could not be applied to observations of [WS99]2, because they consisted of only a limited number of single frames. The object spectra were then extracted from user defined apertures. A linear fit to the background (below $\approx 7\%$ of the peak intensity for all clusters) on both sides of the object spectrum was subtracted.

The spectra were wavelength calibrated using observations of arc discharge lamps. An atmospheric calibrator (B5V) was observed and reduced in the same way as the target and used to divide out the atmospheric absorption features from the spectra.

3.2. Reduction of the optical echelle data

Reduction of the UVES data was performed within the echelle spectra reduction environment of IRAF. Reduction included bias subtraction, flat-fielding and extracting the spectrum from user supplied apertures. A background is fit to neighboring regions and subtracted. Also here, the background was below $\approx 7\%$ of the peak intensity for all clusters. This step includes a bad pixel rejection. The full moon was fairly close to the Antennae during the integrations, and its scattered light introduced a solar spectrum into the data. However, this contribution is very effectively removed during background subtraction.

Wavelength calibration required the identification of many lines in the ThAr-spectra for each of the echelle orders which were identified using a line table available from the ESO-UVES web pages. A dispersion function was then fit and applied to the object data. This data set contains each order of the spectrum in a separate channel. These separate channels are combined into one final spectrum covering the total wavelength range. This involves re-gridding of the wavelength axis into equidistant bins and averaging in the overlapping edges of the orders. The spectral resolution obtained is $R \approx 38,000$ across all orders.

3.3. Estimating the Velocity Dispersions

For each spectrum (both the optical and near-IR spectra), we estimated the σ of the broadening function (assumed to be a Gaussian) which best fit the cluster spectrum in the following way. The stellar spectrum (the template spectrum) was broadened with Gaussian functions of variable σ in velocity space. The resulting set of spectra were then compared with the cluster spectrum. The best fit was determined by evaluating χ^2 and then searching for the minimum of the function $\chi^2(v_r, \sigma)$ using a simplex downhill algorithm for the tour through parameter space.

The dynamical cluster mass was then estimated using

$$M = \frac{\eta \sigma^2 r_{hp}}{G} \quad (1)$$

where η is a constant that depends on the distribution of the stellar density with radius, the mass-to-light ratio as a function of radius, etc. For all clusters (NGC 4038/39 and NGC 1487), it varied between 9.2 and 9.7. σ is the stellar velocity dispersion, r_{hp} is the projected half-light radius, and G is the gravitational constant.

[†]IRAF is distributed by the National Optical Astronomy Observatories, which are operated by the Association of Universities for Research in Astronomy, Inc., under cooperative agreement with the National Science Foundation.

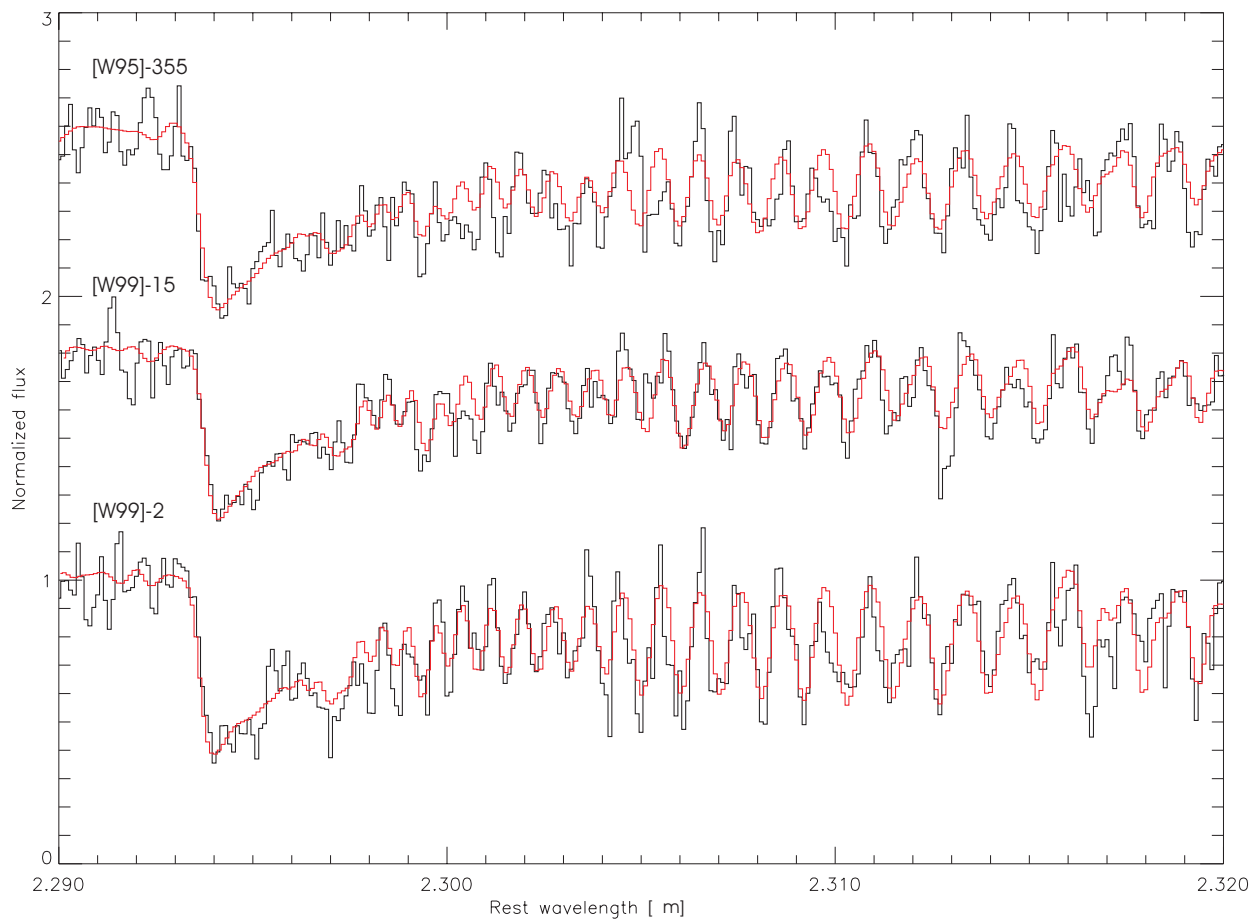


Figure 3. ISAAC Spectra of the three clusters [WS95]355, [W99]15 and [W99]2 (top to bottom, black) with best fits (grey). The bottom plot shows the residuals of the fit to spectrum [W99]15 for the best fit and for two fits with lower and higher velocity dispersions. This gives a visual impression of how much the velocity dispersion affects the spectral features.

Obviously, the template spectrum has to be a good overall match to the cluster spectrum, otherwise an erroneous velocity width will be derived for the cluster. For a star cluster that formed ~ 10 Myrs ago, late K through early M supergiants are expected to provide the largest contribution to the flux at $2.3\mu\text{m}$. However, according to population synthesis models,¹¹ there will be a non-negligible contribution to the flux from hot main sequence stars. Since the stars are hot (O and B-type stars), this “diluting continuum” will be an essentially featureless continuum which solely decreases the equivalent width of the CO band-heads. This has the effect of shifting the apparent dominating stellar type towards higher effective temperatures. Starting out with a template spectrum with weak CO features leads to very low velocity dispersions, the opposite is the case if an M5I star (strong band-heads) is used, with vast differences in the results (a few km s^{-1} to up to about 30 km s^{-1}). For details on how this problem was handled see Mengel et al 2002.¹³

The determination of the velocity dispersion for the optical echelle data used the same procedure as for the ISAAC spectra, relying on the Calcium Triplet around 8500\AA , but also using the Mg absorption feature at 8800\AA and other weaker metal absorption lines between 8400 and 9000\AA .

Examining the spectra in detail, it was obvious that they are composed of a mixture of light from supergiants and hot main sequence stars (the latter adding some Paschen absorption features to the spectrum). This means that the spectra cannot be simply fit by broadening the stellar template, but that either the hot star contribution needs to be added to the template, as was done in the case of the ISAAC spectra, or that the contribution needs to be subtracted from the cluster spectrum. We followed the latter procedure, but found that it does not affect the results which of these two methods is applied.

Cluster [W99]2 was observed with both instruments, ISAAC and UVES, in order to check the consistency of the results. The agreement was excellent ($\sigma = 14.0 \pm 0.8 \text{ km/s}$ from ISAAC and $\sigma = 14.3 \pm 0.5 \text{ km/s}$ from UVES), revealing no systematic offsets between the two instruments/wavelength ranges.

3.4. Estimating the Sizes of the Observed Clusters

In order to make an estimate of the mass, it is necessary to have a measure of the cluster radius and profile shape (see equation 1). We used the archival HST I-band image obtained by Whitmore et al. (1999)⁵ for that purpose for the Antennae, and the I-band HST image which was obtained for Zepf et al. (unpublished) for NGC 1487. Most clusters were slightly-to-well-resolved, and we used the *ishape* routine described by Larsen¹⁴ implemented in the BAOLAB data reduction package developed by Larsen to fit the cluster light profiles with King¹⁵ profiles of different concentrations (we also tried other theoretical cluster profiles, but King15 - King100 models provided the best fits).

For cluster NGC 1487-3, the K-band photometry is complicated by the fact that there is a second, slightly fainter cluster so close by that the two are only marginally separated in our near-IR images. We noticed this fact before we obtained the spectra and always positioned the slit on the brighter of the two clusters, but the large uncertainty in the photometry is due to this. Recently, we obtained HST-ACS images which are intended to improve the size estimates for the clusters in NGC 1487 and several other merging galaxies which are part of our program.

The results of our velocity dispersion and size estimates, together with the resulting dynamical masses and light-to-mass ratios are summarized in Table 3.4.

4. RESULTS

Our results are summarized in Table 3.4. We find a range of cluster velocity dispersions from about 8 km s^{-1} to over 20 km s^{-1} . One concern about any such measurements is the reliability of the final results. For the optical echelle data, the instrumental resolution, $\sigma_{instrument} = 3.2 \text{ km s}^{-1}$ ensures that the cluster line profiles are always well-resolved. The situation for the near-IR data is less clear. For the clusters where the velocity dispersions were estimated from the near-IR CO band-head, the measured values are above or approximately at the instrumental resolution ($\sigma_{instrument} = 14.2 \text{ km s}^{-1}$) and are thus likely to be secure. For some tests that were performed on the reliability of these data, see Mengel et al., 2002.¹³

Table 1. The cluster masses as they were derived from the ISAAC and UVES spectra (in column “Inst.” indicated by I and U, respectively) in comparison with the supergiant template spectrum. The age was derived from the combination of $W_{Br\gamma}$, W_{CO} , and W_{CaT} . The size is the projected half-light radius r_{hp} (for the cluster marked with ^a, we could not obtain a satisfactory fit and used the value kindly provided by B. Whitmore). The stellar velocity dispersion σ is the average value from ISAAC and UVES for [W99]2. M_{vir} is the Virial mass determined from equation 1 with the 1σ -uncertainties given in column σ_M . The light-to-mass ratios were derived from the extinction corrected magnitudes and distance moduli of 31.41 and 30.13 for NGC 4038/4039 and NGC 1487, respectively.

Cluster	Inst. I/U	$m_K(0)$ mag	Age [10^6 yr]	σ [km/s]	r_{hp} [pc]	$\log M_{vir}$ [M_\odot]	σ_M [%]	$\log L_K/M$ [L_\odot/M_\odot]
[WS95]355	I	15.4±0.1	8.5±0.3	21.4±0.7	4.8±0.5 ^a	6.67	12	1.05
[W99]15	I	15.8±0.1	8.7±0.3	20.2±0.7	3.6±0.5	6.52	16	1.09
[W99]2	I/U	14.0±0.1	6.6±0.3	14.2±0.4	4.5±0.5	6.31	12	2.00
[W99]1	U	14.7±0.1	8.1 ±0.5	9.1±0.6	3.6±0.5	5.81	19	2.22
[W99]16	U	15.5±0.1	10±2	15.8±1	6.0±0.5	6.51	15	1.20
unknown	I	15.8±0.1	8.0 ±0.5	8.0±0.7	6.0±0.5	5.93	20	1.49
[W93]331?	I	16.4±0.1	8.1±2.0	9.0±0.7	2.9±0.5	5.72	20	1.51
NGC 1487-1	I	15.5±0.2	8.1±0.5	17.5±1.2	2.3±0.5	6.18	30	1.04
NGC 1487-2	I	15.6±0.2	8.5±0.5	16.4±1.5	1.8±0.5	6.00	32	1.12
NGC 1487-3	I	16.4±0.4	7.9±0.5	20.0±1.5	2.6±0.5	6.36	32	0.50

5. DISCUSSION AND IMPLICATIONS

The underlying assumption of any mass estimate using the velocity dispersion will be that the cluster is self-gravitating (i.e., bound). This assumption we find confirmed from our results, because from the velocity dispersions and half-light radii we estimate that the crossing times ($t_{cross} \sim r_{hp}/\sigma$) range from about 1 to a few $\times 10^5$ yrs. Since the ages of the clusters are around 8 Myrs, they have already survived for 20-50 crossing times and are therefore very likely to be bound, at least initially since subsequent dynamical evolution and mass loss through massive star winds and supernova explosions may unbind the clusters.

One of the critical parameters to understanding star-formation in and the dynamical evolution of these compact, young star-clusters is their initial mass function. If we find that these clusters are best described as having an IMF with significant numbers of low mass stars (say Salpeter slope down to $0.1 M_\odot$), then the dynamical evolution will be driven through the ejection of these numerous low mass stars by binaries and massive stars in the cluster. Moreover, the fraction of the total mass lost through stellar winds and supernova explosion will be relatively small (10s of percent¹¹). It is then likely, since the amount of overall ejected mass is relatively small compared to the total mass, for the clusters to remain bound and long-lived. If however, there is a lack or relative deficit of low mass stars (either through an IMF that is truncated at the low mass limit or that has a relatively flat slope), then the total mass loss from the cluster due to stellar ejection (since higher mass stars would then be more likely to get ejected) and the fraction of the total mass lost through stellar winds and supernova would also be proportionally higher both of which would tend to increase the likelihood that a cluster becomes unbound.¹⁶⁷

In the following we use the derived masses and ages, in combination with the photometry and extinction estimates, to constrain the IMFs of these clusters through the use of population synthesis models. The approach uses a comparison of the cluster with population synthesis models that predict the mass-to-light ratios as a function of the cluster age: The observed light-to-mass ratio compared to theoretical models of different IMF slopes and/or low-mass cutoffs, thereby revealing the low mass star content of the cluster. However, since we are measuring the total mass, there is a degeneracy whether IMF slope or low mass cutoff are responsible for the presence or absence of low mass stars in a cluster.

Figure 5 shows our results for the clusters in NGC 4038/39 and in NGC 1487, together with Starburst99 models of different IMF slopes (the lower mass cutoff was kept constant at $0.1 M_\odot$). In this plot of the $\log L_K/M$ versus age, the most striking feature is that the clusters form two groups: two clusters have L_K/M at

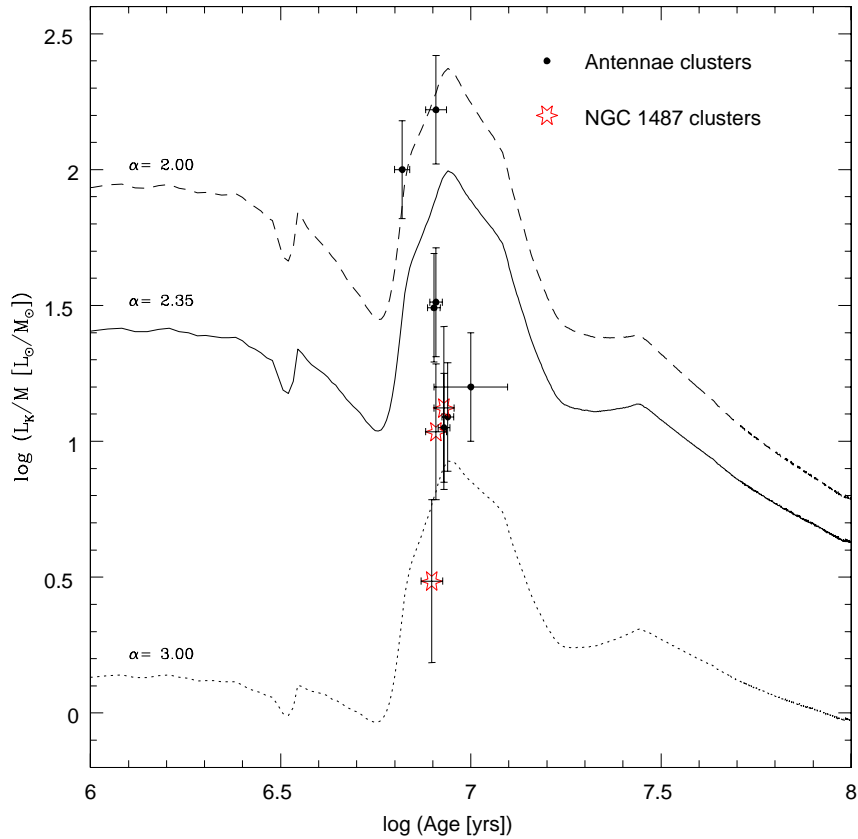


Figure 4. The K-band light-to-mass ratios for the young compact clusters in the Antennae and NGC 1487 compared with models of Leitherer et al. (1999)¹¹ for an instantaneous burst of total mass $10^6 M_{\odot}$ with a power-law slope, and a mass range from 0.1 to $100 M_{\odot}$. The power-law exponent of the slopes are labelled. Points represent the data for clusters with ground-based K-band photometry from ISAAC and SOFI images (Mengel et al. 2002, in preparation) and with the extinction estimated from the ratios $H\alpha / Br\gamma$ in comparison with the expected value and from broadband colors. The error bars represent a combination of the error in the mass and the uncertainty in the photometry. The model light-to-mass ratios shown take into account the mass lost through stellar winds and supernovae over time.

their estimated ages that seem best described with an IMF having a relatively flat slope, while most clusters are consistent with having an IMF slightly steeper than Salpeter. This is true for a lower mass cutoff of $0.1 M_{\odot}$. An alternative description would be to keep the IMF slope fixed (for example at the Salpeter value): then the two clusters which are deficient in low mass stars would have a lower mass cutoff at $1.0 M_{\odot}$, while for the other group, the IMF extends below $0.1 M_{\odot}$.

If the segregation of the cluster points in Figure 5 is a real effect, it means that the IMF varies significantly between clusters. We do not yet have the possibility to disentangle lower mass cutoff and IMF slope, but the two different groups of clusters differ in their ratio of low- to high mass stars by approximately a factor 5 (“low” and “high” relating to stars below and above $3 M_{\odot}$, respectively).

While it is not yet clear whether the observed IMF variations will continue to be seen in different galaxies and environments (while differences are seen amongst the Antennae clusters, all three NGC 1487 clusters are rich in low-mass stars), a discussion of the potential origin of IMF differences might be useful.

The most attractive hypothesis is that perhaps the difference in the relative number of low mass stars is related to the environment in which the cluster is born. Clusters [W99]15 and [WS95]355 suffer greater extinction on average than most clusters in the Antennae and both lie in the over-lap region of the two merging disks. Clusters [W99]1 and [W99]2 lie in the “western loop” of the Antennae’s northern most galaxy, NGC4038 and have relatively low extinctions ($A_V \approx 0.3$ magnitudes). In spite of the clusters having similar ages, the environments of [W99]15 and [WS95]355 appear to be much more rich in dust and gas.^{17,18,10} However, cluster [W99]16, while physically lying near the clusters [W99]15 and [WS95]355, appears to suffer much less extinction (also, the three clusters in NGC 1487 seem to have a rather low extinction). Presumably, since the region where [W99]15, [W99]16, and [WS95]355 were formed is also the region where the two disks are interacting, the gas pressure (both the thermal and turbulent) would be high due to dynamical interactions of the two interstellar media. The local thermal Jeans mass, which is considered to play a role in setting the mass scale for low mass stars¹⁹ is proportional to $T^2 P^{-1/2}$, where T and P are the total pressure and temperature.²⁰ Clouds with low temperature and/or high pressures would form clusters with IMFs weighted towards low mass stars, which would be applicable for the more extinguished clusters. Conversely, clouds that are collapsing in relatively low extinction, gas poor, more quiescent regions might be influenced by the ionizing radiation of nearby young clusters raising its gas temperature. Thus studies of young compact clusters in the Antennae and other galaxies appear to agree with the expectation from the low mass scaling set by the Jeans mass.

Obviously using compact, young star clusters in nearby mergers to provide observational constraints on the processes that lead to the characteristics of the IMF will require much more observational and theoretical work. However, even the relatively sparse and modest results provided here and in the literature are tantalizing and show the promise of this type of observation in advancing our understanding of the process of cluster- and star-formation.

Do these results give an answer to our initial question whether the clusters evolve into globular clusters? Well, only partially. A more definitive answer can only be given if a large number of clusters or an almost complete population of clusters is analyzed, together with, for example, information about the gravitational potential (and its changes) in the merger in which the clusters are formed.

However, the cluster survival probability is strongly dependent on its low-mass stellar content and its concentration, as was shown by various models.²¹ Perhaps the most relevant for this study are those that employ the Fokker-Planck approximation in solving the dynamics of the constituent cluster stars.^{22,16,7} These models suggest the most likely survivors are those clusters that are either more highly concentrated (King model concentrations of greater than 1.0-1.5), and/or those with steep IMFs. This is shown graphically in Fig. 5, where we have reproduced approximately a figure from Takahashi & Portegies Zwart (2000)⁷ (their Figure 8) that shows which range of cluster parameters the clusters are long-lived or disrupt. For the range of plausible IMF slopes that we have determined (assuming, as in the models, that the IMF extends down to sub-solar masses), the models suggest that clusters that are about as concentrated as we have observed in our two analyzed mergers will survive for at least a few Gyrs. Even though we have no independent constraint on the lower mass limit of the stellar mass function, it is interesting that models with steep IMF slopes are also robust against disruption. From these models alone it is difficult to tell if the clusters are able to withstand the disruptive tendencies of the

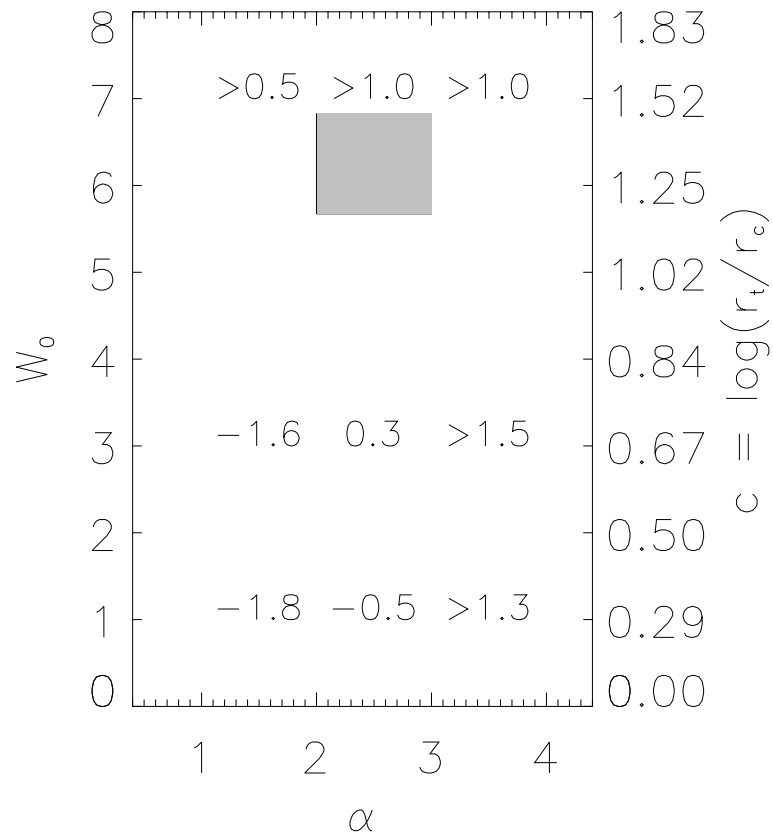


Figure 5. This is a modified reproduction of a figure from Takahashi & Portegies Zwart (2000⁷; their Figure 8) showing the ages at the endpoint of evolution for modeled clusters. The clusters were characterized by scaled central potentials, W_0 (which is related to the concentration, c , as shown in the ordinate on the right side) and IMF slopes (α). The numbers in the grid give the ages at the endpoint of the evolution (disruption or core collapse) as $\log(\text{age [Gyrs]})$. Clusters with values below 0.3 (corresponding to 2 Gyrs) were disrupted by dynamical processes over time, the others experienced core collapse. The grey box shows the region where the clusters in the Antennae and NGC 1487 are observed to lie. This suggests that the clusters are relatively long lived.

large mass loss they suffer if the lower mass limit is raised and the IMF slope steepened, such that the observed light-to-mass ratio constraints are met. The limited number of models so far generated seems to indicate that clusters with very steep slopes ($\alpha > 3$) of their IMF are robust. More modeling is obviously needed to answer this question quantitatively and definitively.

Even if the clusters survive, it is obviously important to have some indication of how much mass loss they may undergo as they age. For some of the cluster parameters, these models suggest that these clusters may lose significant amounts of mass (>50%, sometimes much greater⁷). Clusters with steep IMF slopes ($\alpha > 2.5$) which are compact ($c > 1.5$) apparently suffer large mass loss – may lose more than 90% of their total initial mass.⁷ Therefore, it is easily possible for these cluster to survive, but over their lifetimes, they will have much lower masses than when they are as young as the clusters we have observed here. It is through such strong mass loss that the young compact, very massive clusters in the both mergers may evolve into something similar to the population of clusters observed in galaxies generally.²³²⁴

REFERENCES

1. J.A. Holtzman et al. *Planetary Camera observations of NGC 1275 - Discovery of a central population of compact massive blue star clusters*, AJ, 103, 691, 1992,
2. B.C. Whitmore, F. Schweizer, C. Leitherer, K. Borne, & C. Robert, C. *Hubble Space Telescope discovery of candidate young globular clusters in the merger remnant NGC 7252*, AJ, 106, 1354, 1993
3. G.R. Meurer, T.M. Heckman, C. Leitherer, A. Kinney, C. Robert, & D.R. Garnett *Starbursts and Star Clusters in the Ultraviolet*, AJ, 110, 2665, 1995
4. B.C. Whitmore, B.W. Miller, F. Schweizer, & S.M. Fall *Hubble Space Telescope Observations of Two Dynamically Young Elliptical Galaxies* AJ, 114, 2381, 1997
5. B.C. Whitmore, Q. Zhang, C. Leitherer, M.S. Fall, F. Schweizer, & B.W. Miller, *The luminosity function of young star clusters in "the Antennae" galaxies (NGC 4038/4039)*, AJ, 118, 1551, 1999
6. S.E. Zepf, K.M. Ashman *The Formation and Evolution of Candidate Young Globular Clusters in NGC 3256* AJ, 118, 752, 1999
7. K. Takahashi & S.F. Portegies Zwart *The Evolution of Globular Clusters in the Galaxy* ApJ, 535, 759, 2000
8. W.E. Harris *Globular cluster systems in galaxies beyond the Local Group*, ARA&A, 29, 543, 1991
9. Q. Zhang & S.M. Fall *The Mass Function of Young Star Clusters in the "Antennae" Galaxies* ApJ, 527, 81, 1999
10. S. Mengel, M.D. Lehnert, N.A. Thatte, L.E. Tacconi-Garman, & R. Genzel *K-Band Spectroscopy of Compact Star Clusters in NGC 4038/4039* ApJ, 550, 280, 2001
11. C. Leitherer et al. *Starburst99: Synthesis Models for Galaxies with Active Star Formation*, ApJS, 123, 3, 1999
12. G. Bruzual & S. Charlot *Spectral evolution of stellar populations using isochrone synthesis*, ApJ, 405, 538, 1993
13. S. Mengel, M.D. Lehnert, N.A. Thatte, & R. Genzel *Dynamical masses of young star clusters in NGC 4038/4039* A&A, 383, 137, 2002
14. S.S. Larsen *Young massive star clusters in nearby galaxies. II. Software tools, data reductions and cluster sizes*, A&AS, 139, 393, 1999
15. I.R. King *The structure of star clusters. III. Some simple dynamical models*, AJ, 71, 64, 1966
16. D.F. Chernoff & D.M. Weinberg *Evolution of globular clusters in the Galaxy*, ApJ, 351, 121, 1990
17. B.C. Whitmore & F. Schweizer *Hubble space telescope observations of young star clusters in NGC-4038/4039, 'the Antennae' galaxies*, AJ, 109, 960, 1995
18. C.D. Wilson, N. Scoville, S.C. Madden & V. Charmandaris *The Mass Function of Supergiant Molecular Complexes in the Antennae Galaxies*, ApJ, 542, 120, 2000
19. R.B. Larson *The Stellar Initial Mass Function*, in Proceedings of Star Formation 1999 ed. T. Nakamoto, (Nobeyama Radio Observatory), p. 336, 1999
20. L. Spitzer, Jr. *Physical Processes in the Interstellar Medium*, Wiley-Interscience: New York, 1978
21. L. Spitzer *Dynamical Evolution of Globular Clusters*, Princeton: Princeton Univ. Press, 1987
22. H. Cohn *Numerical integration of the Fokker-Planck equation and the evolution of star clusters*, ApJ, 234, 1036, 1979
23. U. Fritze-v.Alvensleben *Young star clusters in the Antennae: a clue to their nature from evolutionary synthesis*, A&A, 336, 83, 1998
24. U. Fritze-v.Alvensleben *The mass function of Young Star Clusters in the Antennae*, A&A, 342, L25, 1999